

The loss of the PDE6 deactivating enzyme, RGS9, results in precocious light adaptation at low light levels

Andrew Stockman

Institute of Ophthalmology, University College London,
London, UK



Hannah E. Smithson

Department of Psychology, Durham University,
Durham, UK



Andrew R. Webster

Moorfields Eye Hospital,
London, UK



Graham E. Holder

Moorfields Eye Hospital,
London, UK



Naheed A. Rana

MRC Epidemiology Unit, Strangeways Research
Laboratory, Wort's Causeway, Cambridge, UK



Caterina Ripamonti

Institute of Ophthalmology, University College London,
London, UK



Lindsay T. Sharpe

Institute of Ophthalmology, University College London,
London, UK



The GTPase activating protein, RGS9-1, is vital for the deactivation and regulation of the phototransduction cascade (C. K. Chen et al., 2000; C. W. Cowan, R. N. Fariss, I. Sokal, K. Palczewski, & T. G. Wensel, 1998; W. He, C. W. Cowan, & T. G. Wensel, 1998; A. L. Lyubarsky et al., 2001). Its loss through genetic defects in humans has been linked to a slow recovery to changes in illumination (K. M. Nishiguchi et al., 2004). Such a deficit is to be expected because RGS9-1 normally speeds up the deactivation of the activated phosphodiesterase effector molecule, PDE6*, and thus accelerates the turning off of the visual response. Paradoxically, however, we find that the cone response in an observer lacking RGS9-1 is faster at lower light levels than it is in a normal observer. Though surprising, this result is nonetheless consistent with molecular models of light adaptation (e.g., E. N. Pugh, S. Nikonov, & T. D. Lamb, 1999), which predict that the excess of PDE6* resulting from the loss of RGS9-1 will shorten the visual integration time and *speed up* the visual response at inappropriately low light levels. The gain in speed caused by the superfluity of PDE6* at lower light levels compensates for the loss caused by its slow deactivation; thus quickening the response relative to that in the normal. As the light level is increased and the PDE6* concentration in the normal rises relative to that in the observer lacking RGS9-1, the temporal advantage of the latter is soon lost, leaving only the deficit due to delayed deactivation.

Keywords: vision, cone photoreceptor, visual transduction, photopigment, bradyopsia, RGS9, PDE6, light adaptation

Citation: Stockman, A., Smithson, H. E., Webster, A. R., Holder, G. E., Rana, N. A., Ripamonti, C., & Sharpe, L. T. (2008). The loss of the PDE6 deactivating enzyme, RGS9, results in precocious light adaptation at low light levels. *Journal of Vision*, 8(1):10, 1–10, <http://journalofvision.org/8/1/10/>, doi:10.1167/8.1.10.

Introduction

The visual response is initiated by the absorption of a photon, which transforms rhodopsin (R) into its activated form (R*). R* then catalyzes the exchange of guanosine diphosphate (GDP) for guanosine triphosphate (GTP) on the alpha-subunit of the G-protein transducin ($G\alpha$), resulting in the separation of the active trimer ($G\alpha^*$ or

$G\alpha$ -GTP). $G\alpha^*$ in turn activates the phosphodiesterase effector molecule (PDE6*), by exposing sites that catalyze the hydrolysis of cyclic guanosine monophosphate (cGMP) into GMP. The reduction in cGMP closes cyclic-nucleotide-gated (CNG) channels in the plasma membrane, thus blocking the inward flow of Na^+ and Ca^{2+} ions and causing hyperpolarization (see Figure 1; and for reviews and models, see, e.g., Arshavsky, Lamb, & Pugh, 2002; Burns & Baylor, 2001; Hamer, Nicholas, Tranchina,

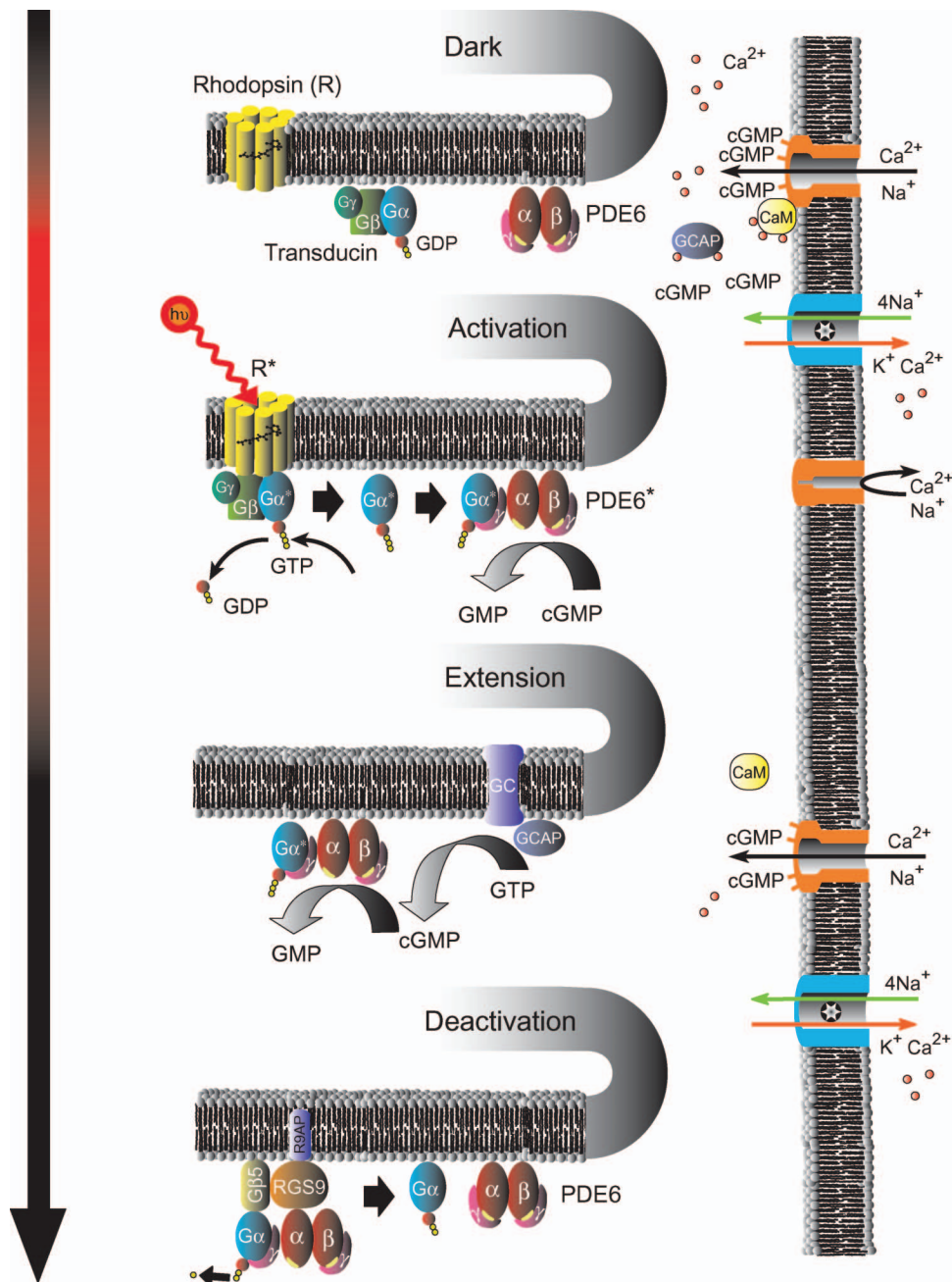
Lamb, & Jarvinen, 2005; Pugh & Lamb, 2000; Pugh, Nikonov, & Lamb, 1999).

To turn off the visual response, each of the activated molecules has to be deactivated. $G\alpha^*$ and $PDE6^*$ are simultaneously deactivated by the hydrolysis of the $G\alpha^*$ -bound GTP to GDP. This GTPase activity is substantially accelerated by RGS9-1 (Cowan, Fariss, Sokal, Palczewski, & Wensel, 1998; He, Cowan, & Wensel, 1998), a GTPase activating protein (GAP) that binds to the $G\beta 5$ subunit (Makino, Handy, Li, & Arshavsky, 1999) and to R9AP, a membrane anchor (Hu & Wensel, 2002).

Our work focuses on the visual deficits in a rare subject with specific mutations in the genes encoding the RGS9-1 enzyme. The absence of this enzyme has been demonstrated *in vivo* to cause slow recovery to abrupt changes in

illumination both in knock-out mice lacking RGS9-1 in their photoreceptor outer segments (Chen et al., 2000; Krispel, Chen, Simon, & Burns, 2003; Lyubarsky et al., 2001) and in human observers with gene defects affecting either RGS9-1 or R9AP (Nishiguchi et al., 2004). These results are consistent with previous evidence suggesting that the absence of RGS9-1 or R9AP drastically slows down the deactivation of $PDE6^*$, and thus the visual response—changes that have led to the visual deficit being referred to as bradyopsia (or “slow” vision) (Nishiguchi et al., 2004).

Another important consequence of the slowed deactivation of $PDE6^*$ seems to have been overlooked, however. The resulting increase in the intracellular concentration of $PDE6^*$ (which is normally produced by



increasing light levels) will increase the rates of removal and replacement of cGMP (see “Extension” in Figure 1), an increase which is thought to be one of the principal mechanisms by which the visual system shortens its visual integration time and speeds up its visual response as the light level increases (Hodgkin & Nunn, 1988; Nikonov, Engheta, & Pugh, 1998; Pugh et al., 1999). According to this molecular model, the excess of PDE6* in bradyopsia patients should lead to a speeding up of their visual response at inappropriately low light levels. By making a detailed comparison between vision in normal observers and in an observer lacking RGS9-1, we investigate whether this speeding up can be quantified psychophysically. Over a limited range of low light levels, we demonstrate that precocious light adaptation in the affected observer compensates for the losses caused by slow deactivation, so that his visual response is actually faster than normal.

Methods

Subjects

A 62-year-old male, initially identified by his abnormal electroretinographic recordings, served as the affected observer. Retinal examination was normal. Visual acuities were 0.5 in each eye with a hyperopic correction. Color vision as determined by standard tests (Farnsworth–Munsell 100-hue, Rayleigh and Moreland anomaloscope matches, and Ishihara plates) was normal. Analysis of the coding region of the RGS9 gene confirmed compound heterozygosity for the previously described missense mutation (p.W299R, c.895T → C) and a novel nonsense mutation (p.R128X, c.382C → T), which together imply the complete absence of the functional protein from the retina (Rana, Saihan, O’Toole, Hykin, Richardson, Robson, Holder, & Webster, manuscript in preparation). After a period of training, the affected observer made highly consistent and reproducible psychophysical settings.

Four male (aged 49, 50, 55, and 62) and one female (aged 36) normal control subjects were used (mean age 50). The study conforms to the standards set by the Declaration of Helsinki, and the procedures were approved by local ethics committees at Moorfields Eye Hospital and at University College London.

Apparatus

A computer-controlled Maxwellian-view optical system with a 2-mm entrance pupil illuminated by a 900-W Xe arc was used for these experiments. Wavelengths were selected by the use of interference filters with full-width at half-maximum bandwidths of between 7 and 11 nm

(Ealing or Oriel). The radiance of each beam could be controlled by the insertion of fixed neutral density filters (Oriel) or by the rotation of circular, variable neutral density filters (Rolyn Optics). Sinusoidal modulation was produced by pulse-width modulation of fast, liquid crystal light shutters (Displaytech) at a carrier frequency of 400 Hz (which is itself much too fast to be visually resolved). The position of the observer’s head was maintained by a dental wax impression. This system is described in more detail elsewhere (Stockman, Plummer, & Montag, 2005).

Stimuli

The experimental conditions were chosen to measure the temporal properties of either the S-cones or the L- (and M-) cones.

Figure 1. Dark: The chromophore molecule, 11-*cis*-retinal, lies in the pocket formed by the seven trans-membrane helices of the G-protein-coupled-receptor-protein rhodopsin (R). Both the G-protein transducin ($G\alpha$ -GDP- $G\beta$ - $G\gamma$) and the tetrameric effector enzyme phosphodiesterase (PDE6) are in their inactive states; and the intracellular concentration of cGMP is relatively high. cGMP is thus able to bind to and open cyclic-nucleotide-gated (CNG) channels in the plasma membrane, through which Ca^{2+} and Na^{+} ions flow into the cell. Activation: The absorption of a photon isomerizes the chromophore to its *all-trans* form and triggers a conformational change of the rhodopsin into its activated state (R^*). R^* then activates transducin by catalyzing the exchange of GDP for GTP, which causes the separation of activated α -transducin ($G\alpha^*$) from the trimer. $G\alpha^*$ in turn activates the phosphodiesterase enzyme (PDE6*) by exposing a site that catalyzes the hydrolysis of cGMP into GMP. The decreased cGMP concentration results in the loss of cGMP from the CNG channels, which close, blocking the inward flow of Na^{+} and Ca^{2+} ions, reducing the circulating electrical current, and hyperpolarizing the membrane voltage. Extension: Two [Ca^{2+}] sensitive mechanisms extend the visual response in light. First, cGMP is restored by retinal guanylate cyclase (GC), the activity of which is enhanced by guanylate cyclase activating protein (GCAP). Since GCAPs are inactivated by bound Ca^{2+} ions (top), their ability to enhance GC increases as the [Ca^{2+}] falls. Second, the sensitivity of CNG channels to cGMP is increased when calmodulin (CaM) dissociates from the channels as its Ca^{2+} ions are lost. Deactivation: Both $G\alpha^*$ -PDE6* are simultaneously deactivated by the hydrolysis of the attached GTP to GDP. This GTPase activity is substantially enhanced by the GTPase-activating proteins (GAP) RGS9-G β 5, which are attached to the R9AP membrane anchor protein. This illustration is inspired by Figure 1 of Pugh et al. (1999) and by Figure 2 of Burns and Arshavsky (2005). Further details of the cascade processes and references can be found in one of many reviews (see Arshavsky et al., 2002; Burns & Arshavsky, 2005; Burns & Baylor, 2001; Fain, Matthews, Cornwall, & Koutalos, 2001; Hamer et al., 2005; Perlman & Normann, 1998; Pugh & Lamb, 2000; Pugh et al., 1999).

S-cone measurements

A flickering target of 4° of visual angle in diameter and 440 nm in wavelength was presented in the center of a 9° diameter background field of 620 nm. Fixation was central. The 620-nm background field selectively desensitized the M- and L-cones but had comparatively little direct effect on the S-cones. For the normal observers, a 620-nm field of $11.51 \log_{10} \text{ quanta s}^{-1} \text{ deg}^{-2}$ was used, which isolates the S-cone response up to a 440-nm target radiance of about $10.5 \log_{10} \text{ quanta s}^{-1} \text{ deg}^{-2}$ (e.g., Stockman, MacLeod, & DePriest, 1991; Stockman, MacLeod, & Lebrun, 1993; Stockman & Plummer, 1998). For the -RGS9-1 observer, who complained that this background dazzled him, a dimmer field of $10.26 \log_{10} \text{ quanta s}^{-1} \text{ deg}^{-2}$ was used. This lower radiance still sufficed to maintain his S-cone isolation (see also Figure 2 and associated text below).

L-cone measurements

A flickering target of 4° of visual angle in diameter and 650 nm in wavelength was presented in the center of a 9° diameter background field of 481 nm. Fixation was again central. The 481-nm background, which delivered $8.26 \log \text{ quanta s}^{-1} \text{ deg}^{-2}$ at the cornea ($1.39 \log$ photopic trolands or $2.53 \log$ scotopic trolands), mainly served to saturate the rods but also selectively desensitized the M-cones at lower target radiances. The primary target wavelength of 650 nm was chosen to favor detection by cones rather than rods. It was varied in intensity in the critical flicker fusion (c.f.f.) measurements (see Procedures) from 6.5 or 7.0 to $11.5 \log_{10} \text{ quanta s}^{-1} \text{ deg}^{-2}$ (to convert to \log photopic trolands subtract 7.13 from the 650-nm \log quantal values). These conditions isolate the L-cone response over most of the 650-nm intensity range; but at high intensities, the M-cones are also likely to contribute to flicker detection. We were not concerned about the possibility of a mixed M- and L-cone response at higher levels.

Procedures

An efficient way of assessing the effects of light adaptation is to characterize the changes in temporal sensitivity that accompany changes in adaptation level. We therefore measured, as a function of light level, changes in temporal acuity or resolution (also known as the critical flicker fusion or c.f.f.) and changes in temporal modulation sensitivity.

Before the measurements, both the normal and affected observers light adapted to the background and target for 3 minutes. They interacted with the computer that controls the apparatus by means of buttons and received information and instructions via tones and a computer-controlled

voice synthesizer. Each individual measurement was the average of three settings. The two types of measurements were made as follows.

Critical flicker fusion (or c.f.f.) measurements

Observers adjusted the flicker frequency (at the fixed maximum target modulation of 92%) to find the frequency at which the flicker just disappeared. For the -RGS9-1 observer, the L-cone c.f.f. measurements were also carried out during the cone plateau when the cones have recovered from a bleach but rods have not, to ensure that rods were not contributing to the measurements. The bleach was a white Ganzfeld (full-field) bleach of $5.42 \log \text{ sc td}$ viewed for 30 s, which bleaches approximately 60% of the rod photopigment (Pugh, 1976a; Rushton, 1972). This bleach suffices to elevate rod threshold substantially during the cone plateau and for many minutes thereafter (e.g., Pugh, 1976b). Measurements were made between 3 and 7 minutes after offset of the Ganzfeld.

Modulation threshold measurements

Observers adjusted the flicker modulation (at a series of fixed flicker frequencies from 0.5 to 30 or 40 Hz) to find the modulation at which the flicker just disappeared. L-cone modulation sensitivities were measured in the normal and RGS9-1 observers at fixed time-averaged 650-nm target radiances of 7.45, 8.42, 9.41, and $10.38 \log \text{ quanta s}^{-1} \text{ deg}^{-2}$.

Each data point is the average of three or four independent measurements, each of which is the average of three settings. The error bars are ± 1 standard error of the measurements (*SEM*).

Calibration

The radiant fluxes of test and background fields were measured at the plane of the observer's entrance pupil with a UDT Radiometer that had been calibrated by the manufacturer against a standard traceable to the National Bureau of Standards and cross-calibrated by us. Neutral density filters, fixed and variable, were calibrated *in situ* for all test, and field wavelengths were used. Interference filters were calibrated *in situ* with a spectroradiometer (Gamma Scientific).

Results

Temporal acuity measures

Figure 2A shows how the S-cone-mediated c.f.f. changes with increasing radiance of the 440-nm target for

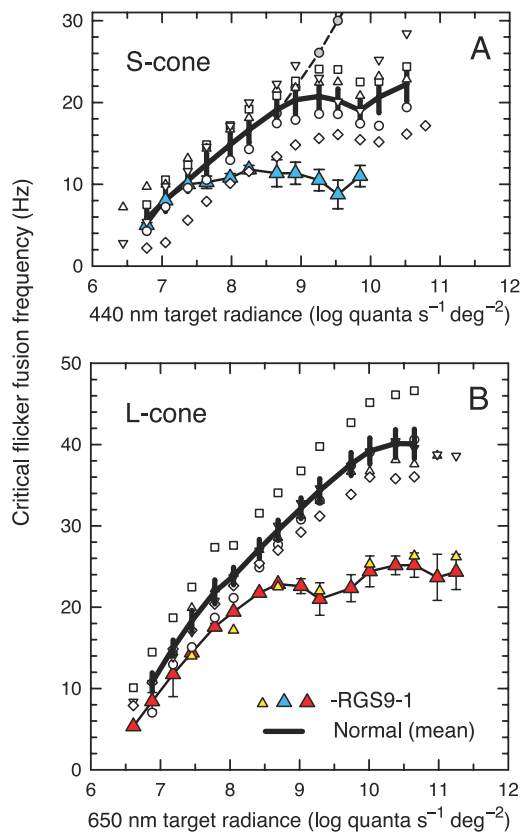


Figure 2. Temporal acuity (c.f.f.) versus intensity functions. S-cone (A) and L-cone (B) c.f.f. data for the $-RGS9-1$ observer (colored triangles) and for five normal observers (open symbols). Each data point is the average of three or four independent measurements, and the error bars (shown only for the $-RGS9-1$ observer) are ± 1 standard error of the measurements. The normal population mean and ± 1 standard error are shown by the thick solid lines. The small gray circles joined by the dashed line in Panel A show c.f.f. data for one observer (whose other c.f.f. data are shown by the open circles) measured at the lower 620-nm background radiance also used by the $-RGS9-1$ observer. The small yellow triangles in Panel B show the c.f.f. data for the $-RGS9-1$ observer measured during the rod-cone plateau following a rod bleach (see [Procedures](#)). Because the two sets of thresholds are the same (red triangles, small yellow triangles), we can conclude that the L-cone c.f.f. function in the $-RGS9-1$ observer is not rod mediated.

five normal observers (open symbols) and for the $-RGS9-1$ observer (blue triangles). The mean and ± 1 standard error for the five normal observers are shown by the thick solid line and error bars. The data for the normal subjects are similar to those reported in other studies (e.g., Marks & Bornstein, 1973; Stockman et al., 1991; Stockman & Plummer, 1998). The normal c.f.f. functions increase steadily over the first 2.5 log units of radiance but then reach a ceiling of 16 to 25 Hz. Thereafter, the c.f.f. falls slightly before rising again at the highest levels. The slight fall is caused by S-cone saturation, while the final rise is due to the M-cones taking over detection above c. $10 \log_{10}$ quanta

$s^{-1} \text{ deg}^{-2}$ (Stockman & Plummer, 1998). By contrast, the S-cone c.f.f. function for the $-RGS9-1$ observer, lies within the normal range up to c. $7.50 \log_{10}$ quanta $s^{-1} \text{ deg}^{-2}$, but reaches a ceiling of approximately 11 Hz at a much lower radiance of the 440-nm target. The maximum S-cone c.f.f. for the $-RGS9-1$ observer is roughly half of the mean for normal observers (11 as compared to 21 Hz).

Because he complained of discomfort at the higher background radiance, a dimmer orange, 620-nm background was used for the $-RGS9-1$ observer. Fortunately, the use of different backgrounds for the two groups does not invalidate the comparison, because the reduction in background radiance in this range has little effect on the shape of the S-cone c.f.f. itself. This is illustrated in [Figure 2A](#) for the normal observer whose S-cone c.f.f. data are shown by the open circles. The small gray circles joined by the dashed line show the c.f.f. that is found if the lower radiance background is used. The sudden increase in slope (at a target radiance of c. $8.75 \log_{10}$ quanta $s^{-1} \text{ deg}^{-2}$) reflects M-cone intrusion. However, below this level the S-cone c.f.f. is relatively unchanged. Thus, the main effect of using the lower radiance background in the normal is to lower the 440-nm target radiance at which flicker detection is first mediated by the M-cones. The abnormally low light-adapted flicker sensitivity of the $-RGS9-1$ observer helps to maintain his S-cone isolation even with the lower radiance 620-nm background.

The normal subject with the lowest S-cone c.f.f.'s (open diamonds) is the 62-year-old subject, who is of the same age as the $-RGS9-1$ subject. His c.f.f. data are similar to the other normal data except they are clearly shifted towards higher target radiances. This shift is to be expected with increasing age, because the lens pigment density increases with age (e.g., Pokorny, Smith, & Lutze, 1988), thus blocking increasing amounts of shortwave light. Interestingly, a comparable shift is not found for the $-RGS9-1$ observer. We speculate that this is because his condition has caused him to avoid exposure to bright sunlight and consequently its potentially damaging effects (see, e.g., West et al., 1998).

[Figure 2B](#) shows how the L-cone-mediated c.f.f. changes with the radiance of the 650-nm target for the five normal observers (open symbols) and the $-RGS9-1$ observer (red triangles). With increasing target radiance, the L-cone c.f.f. for all observers starts to rise just above $6.5 \log_{10}$ quanta $s^{-1} \text{ deg}^{-2}$. For the normal observers, the c.f.f. rises steadily until reaching a plateau of 36 to 47 Hz above about $10.0 \log_{10}$ quanta $s^{-1} \text{ deg}^{-2}$. The normal data are comparable with other measurements (see also, e.g., Hecht & Shlaer, 1936; Hecht & Verrijp, 1933). By contrast, the c.f.f. data for the $-RGS9-1$ observer rise to only 24 Hz and level off at a radiance c. 2 log units below those for the normals. Importantly, though, like the S-cone c.f.f., the L-cone c.f.f. for the $-RGS9-1$ observer initially lies close to the lower limit of the normal range. The small yellow triangles in [Figure 2B](#) show the c.f.f. data for the $-RGS9-1$ observer measured during the rod-cone plateau following a rod bleach

(see [Procedures](#)). Because the two sets of thresholds are the same, we can conclude that the impaired L-cone c.f.f. function in the $-RGS9-1$ observer is not rod-mediated.

Both the S-cone and the L-cone-mediated c.f.f. data illustrate that, at lower radiance levels, adaptation-dependent improvements in temporal resolution in the $-RGS9-1$ observer roughly match those found in normal observers. This presents something of a conundrum: How can the temporal acuity of a patient with an RGS9 mutation, and thus bradyopsia or slow vision, match that of a normal observer?

Temporal modulation sensitivity measures

More information about the nature of the loss in the $-RGS9-1$ observer can be obtained from temporal modulation sensitivity measurements, which characterize the temporal response at frequencies below the c.f.f. [Figure 3](#) shows mean temporal modulation sensitivities measured at four [1]–[4] time-averaged 650-nm target radiances of 7.45 (filled circles), 8.42 (light gray squares), 9.41 (dark gray triangles), and 10.38 (open inverted triangles) log quanta $s^{-1} deg^{-2}$ for the five normal observers ([Figure 3A](#)) and for the $-RGS9-1$ observer ([Figure 3B](#)). The mean normal data are typical for a small target (e.g., De Lange, 1958): above 8.42 log quanta $s^{-1} deg^{-2}$. Increases in radiance cause the modulation sensitivities at low frequencies to fall and those at high frequencies to rise, with the result that the functions become more bandpass (peaked). Such changes are broadly characteristic of a speeding up of the visual response and a shortening of the visual integration time (see Stockman, Langendörfer, Smithson, & Sharpe, 2006). On the other hand, the data for the $-RGS9-1$ observer, as expected from the c.f.f. measurements, are atypical. First, the functions above 8.42 log quanta $s^{-1} deg^{-2}$ are more low-pass (i.e., less peaked) than those of the normal. Second, overall sensitivity is markedly suppressed, except at the lowest adaptation level.

The bottom panel ([Figure 3C](#)) shows the sensitivity losses suffered by the $-RGS9-1$ observer relative to the normal observers. We are particularly interested in the losses as a function of frequency because it is the relative response to low and high temporal frequencies that will reveal changes in the integration time of the visual response. At level [1], the losses increase slightly and then decrease with frequency, with an average loss of only 0.2 log unit. These losses are within the range of normal variability, which suggests, surprisingly, that there is no consistent difference at this level in the speed of response between the normal observers and the $-RGS9-1$ observer. At level [2], the data for the $-RGS9-1$ observer show a relative average loss of sensitivity of 0.55 log unit that is roughly independent of frequency, which suggests no relative speeding up of the normal response between levels [1] and [2]. This similarity in response speed, however, is lost at the next level [3], at which the

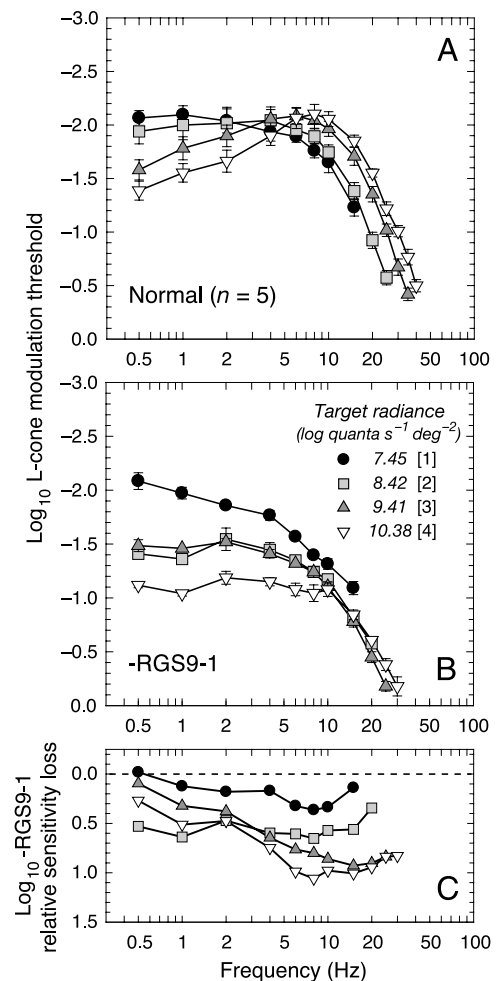


Figure 3. L-cone modulation sensitivities. Mean functions measured at four time-averaged 650-nm target radiances of [1] 7.45 (black circles); [2] 8.42 (light gray squares); [3] 9.41 (dark gray triangles); and [4] 10.38 (inverted triangles) log quanta $s^{-1} deg^{-2}$, for (A) the five normal observers and for (B) the $-RGS9-1$ observer, and (C) differences between the functions plotted as the sensitivity loss for the $-RGS9-1$ observer with the loss increasing downwards. The standard errors are between observers in panel A and between measurements in panel B.

$-RGS9-1$ observer shows a relative decrease in sensitivity with frequency of 0.83 log unit over the frequency range, and this loss is maintained at level [4].

Direct comparisons between the modulation sensitivity data for the mean normal observers and the $-RGS9-1$ observer, such as those shown in [Figure 3C](#), are likely to reflect differences between the two types of observer that are due to factors additional to adaptational changes or to the loss of RGS9-1, such as criterion differences in threshold settings, neural differences arising from the deficit, or other processes. We can focus on the important *differences* caused just by the adaptational changes by plotting the relative changes in sensitivity between successive levels (i.e., the ratios of sensitivities), as shown

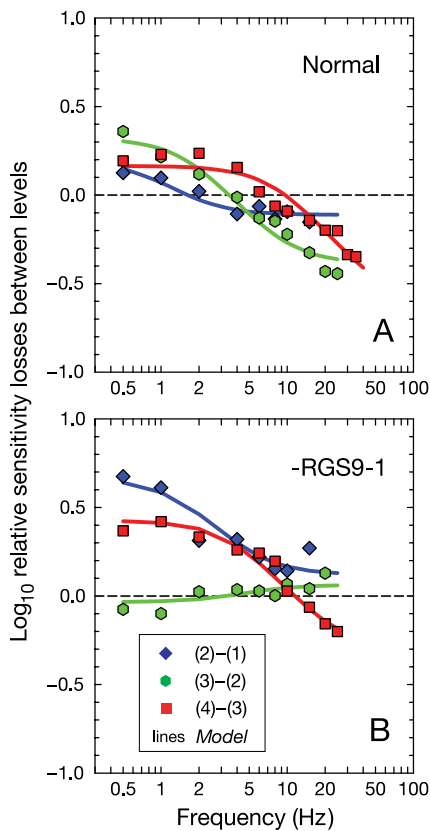


Figure 4. Mean successive sensitivity losses for the normal observers (A) and the $-RGS9-1$ observer (B) *between* levels [2] and [1] (blue diamonds); levels [3] and [2] (green hexagons); and levels [4] and [3] (red squares). The continuous lines in both panels are model fits in which the time constant of a single leaky integrator and the overall sensitivity are allowed to vary. For details, see text.

in Figures 4A and 4B for the normal observers and the $-RGS9-1$ observer, respectively. The differences between the five normal observers and the $-RGS9-1$ observer are striking. Between levels [1] and [2] (blue diamonds), the response of the $-RGS9-1$ observer shows clear evidence of a substantial decrease in integration time and a speeding up of his visual response (i.e., his function has a negative slope showing a relative increase in high-frequency sensitivity), whereas the change for the normal observers is smaller. By contrast, between levels [2] and [3] (green hexagons), the $-RGS9-1$ observer shows no evidence for a decrease in integration time, whereas the normal observers show evidence for a substantial decrease. Lastly, between levels [3] and [4] (red squares), both the normals and the $-RGS9-1$ observer show evidence for a comparable shortening of integration time and associated increases in sensitivity to high frequencies.

These results suggest that, at low light levels, the integration time that underlies the shape of the modulation sensitivity functions can be shorter, and the visual response “faster,” for the $-RGS9-1$ observer than for the normal.

Discussion

Previous visual experiments have been carried out in five human patients with gene defects affecting either RGS9-1 or its anchor protein R9AP (Nishiguchi et al., 2004). The five patients, like our observer, reported difficulties in going from dark to light, such as when walking out of a dimly lit house into bright sunlight. (Nishiguchi et al., 2004). Four of them were homozygous for the missense mutation W299 in the RGS9 gene, while the fifth had a homozygous frameshift mutation R65 in the R9AP gene (Nishiguchi et al., 2004). The patients were found to have diminished white-flash 0.5 and 30 Hz ERGs, and in double-flash ERGs showed a substantial suppression of the second-flash response up to 1 min after the first-flash, in contrast to normals whose second-flash response recovers after 2 s. As noted above, the authors coined the phrase bradyopsia (or slow vision) to describe the visual deficits in these patients (Nishiguchi et al., 2004). Given our results, however, “slowness” needs to be carefully qualified and may not be the most appropriate term to describe the deficit. Indeed, the activation stages of the transduction cascade in the $-RGS9-1$ observer should be as fast as those in the normal observer, as shown by the similar rising phases of the single-flash rod responses in normal rats and in rats lacking G β 5, a G-protein β subunit crucial for the function of RGS9-1 (Krispel et al., 2003). We can estimate the amount by which the integration times shorten for both the normal and the $-RGS9-1$ observer by applying a simple model.

Sensitivity and time constants

It has been common to model the response of the visual system as a cascade of low-pass filters (e.g., Watson, 1986). In terms of phototransduction, this approach is equivalent to considering the system as a cascade of independent reactions having first-order exponential decays. By measuring the *change* in response of the system from one light level to another, we can discount stages of the cascade whose time constants do not change. We find that the data presented in Figure 4—the measured changes in temporal modulation sensitivity from one light level to the next—can be remarkably well described by the changes in the time constant of a *single* first-order reaction (see below). The need for just a single stage is consistent with the molecular analysis by Nikonov, Pugh, and Lamb (2000), who suggested that the decrease in the time constant of hydrolysis of cGMP is the primary mechanism driving the speeding up of the rod photo-response under light adaptation. (Indeed, they argue that the recovery of cGMP concentration will progress exponentially with a rate constant equal to the PDE activity.) Given that the measured changes in temporal modulation sensitivity are consistent with changes in the

time constant of a single first-order reaction, we tentatively relate the changes in our measurements to changes in the rate of cGMP hydrolysis mediated by the light-induced rise in the concentration of PDE6* (Hodgkin & Nunn, 1988; Nikonov et al., 1998). We note, however, that a model with multiple stages (cascaded low-pass filters) would fit our data just as well, so that our data do not preclude multiple mechanisms.

We apply our model by changing the time constant of a leaky integrator or filter, which is comparable to a first order biochemical reaction. In the leaky integrator, the response to a pulse decays exponentially with time; while in the reaction, the concentration of the reactant decays exponentially with time. The standard formula for the amplitude response, $A(f)$, of a leaky integrator is

$$A_n(f) = \tau_n \left[(2\pi f \tau_n)^2 + 1 \right]^{-0.5}, \quad (1)$$

where f is the frequency in Hz, and τ is the time constant in seconds (e.g., Watson, 1986). n , here, refers to the level number from 1 (the lowest) to 4 (the highest). The fits were carried out to the loss data shown in Figures 4A and 4B for each subject by simultaneously finding successive values of τ (τ_1 to τ_4) that would account for the sensitivity losses between each pair of levels, allowing a vertical logarithmic shift (i.e., sensitivity scaling) between them. Put more formally, the fitting equation was

$$\log_{10}[S_n(f)/S_{n-1}(f)] = \log_{10}[A_n(f)/A_{n-1}(f)] + c, \quad (2)$$

where $S_n(f)/S_{n-1}(f)$ is the sensitivity loss between levels n and $n - 1$, $A_n(f)/A_{n-1}(f)$ is the change in amplitude response between those levels (from Equation 1), and c is the logarithmic shift. The fits minimized the squared residuals between the data and the predictions.

The fits, which are shown by the continuous lines in the two panels, color-level coded the same way as the symbols, are very good. For the mean normal observer, the model accounts for 94.34% of the variance; the time constants in milliseconds for successive levels with \pm standard error of the fit are [1]: 188.04 ± 52.41 ; [2]: 92.53 ± 15.08 ; [3]: 18.16 ± 2.48 ; and [4]: 2.95 ± 1.38 , while the logarithmic sensitivity adjustments between levels are [2]–[1]: -0.11 ± 0.02 ; [3]–[2]: -0.39 ± 0.03 ; and [4]–[3]: -0.63 ± 0.16 . For the –RGS9-1 observer, the model accounts for 93.72% of the variance; the time constants in milliseconds for successive levels are [1]: 110.60 ± 26.70 ; [2]: 31.85 ± 6.29 ; [3]: 39.83 ± 6.97 ; and [4]: 7.56 ± 2.53 , while the logarithmic sensitivity adjustments between levels are [2]–[1]: 0.12 ± 0.039 ; [3]–[2]: 0.06 ± 0.03 ; and [4]–[3]: -0.30 ± 0.10 . The standard errors are large for the changes in time constant between

the two lowest levels because the successive time constants are poorly constrained by the data, but the predictions are generally good.

Figure 5 shows the time constants (Figure 5A) and the cumulative gains in sensitivity (Figure 5B) for the –RGS9-1 observer (dotted open circles) and for the mean normal observer (dotted yellow squares) plotted as a function of the mean photopic luminance of the combined target and background. The cumulative sensitivity gains are the cumulative values of c from Equation 2. The changes in time constant and sensitivity for the normal observers are consistent with our earlier work on M- and S-cone adaptation (Stockman et al., 2006; Stockman, Langendörfer, & Sharpe, 2007). In those studies, we also found that light adaptation could be accounted for by shortening time constants accompanied by compensatory increases in overall sensitivity. The overall sensitivity improvements were linked to molecular mechanisms of adaptation that extend the range of the response, such as the increase in the rate of cGMP synthesis mediated by guanylyl cyclase (GC) and the decrease in sensitivity of the CNG channels for cGMP (see Figure 1 and Stockman et al., 2006).

The changes in time constant and sensitivity for the –RGS9-1 observer are consistent with the hypothesis that the excess of PDE6* causes his system to light

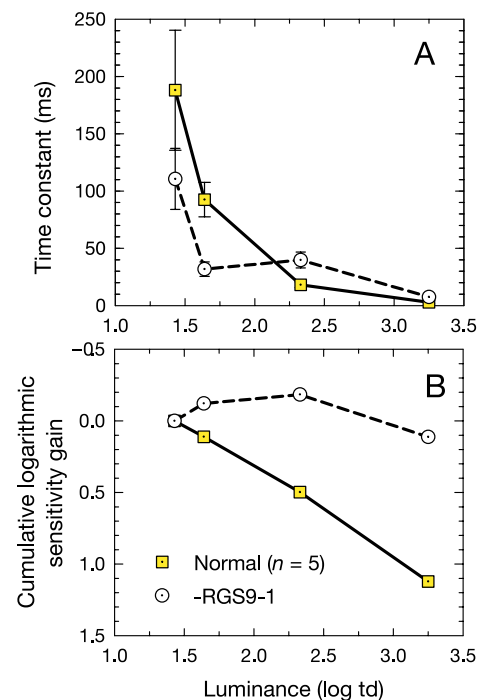


Figure 5. Changing time constants in milliseconds (A) and cumulative sensitivity gains (B) for the normal observers (dotted yellow squares) and the –RGS9-1 observer (dotted open circles) as a function of mean photopic luminance based on model fits. For details, see text.

adapt prematurely. For him, an initially short time constant becomes substantially shorter between the two lowest luminance levels, before reaching an asymptotic value. By contrast, the time constants for the normals shorten more gradually between each successive level. In terms of time constant, the $-RGS9-1$ actually has a temporal advantage over the normal observer at the lowest levels, but that advantage is lost at the highest levels. Significantly, the $-RGS9-1$ observer does not show the sensitivity gains shown by the normal observers. This result suggests that any restoring effects caused by for example cGMP resynthesis has already reached its limiting rate, which is to be expected with an excess of PDE6*.

Interestingly, between the two highest levels, both the normal observers and the $-RGS9-1$ observer show evidence for shortening time constants and sensitivity gains (see Figure 5). This consistency between the two types of observers may reflect a common underlying adaptation mechanism that does not depend upon RGS9-1 (see Krispel et al., 2003; and for discussion of molecular mechanisms related to adaptation, see Pugh et al., 1999; Stockman et al., 2006).

Conclusion

Rare genetic disorders in the essential processes of the phototransduction cascade allow us to analyze *in vivo* components of the human light adaptation process. Here, we have investigated light adaptation in an observer lacking the GTPase activating protein RGS9-1, which speeds up the rate of deactivation of PDE6*. Normally, the concentration of PDE6* is exquisitely balanced, and its catalyzed deactivation maintains visual sensitivity as the light level increases. In this observer, an excess of PDE6* causes light adaptation to be precipitate at inappropriately low light levels.

Acknowledgments

This work was supported by Fight for Sight. We are extremely grateful to the subject, whose voluntary participation and many visits to the laboratory made this work possible. We also thank Jim Bowmaker and Glen Jeffrey for being control subjects.

Commercial relationships: none.

Corresponding author: Andrew Stockman.

Email: a.stockman@ucl.ac.uk.

Address: Institute of Ophthalmology, University College London, 11-43 Bath Street, London EC1V 9EL, England.

References

- Arshavsky, V. Y., Lamb, T. D., & Pugh, E. N., Jr. (2002). G proteins and phototransduction. *Annual Review of Physiology*, *64*, 153–187. [[PubMed](#)]
- Burns, M. E., & Arshavsky, V. Y. (2005). Beyond counting photons: Trials and trends in vertebrate visual transduction. *Neuron*, *48*, 387–401. [[PubMed](#)] [[Article](#)]
- Burns, M. E., & Baylor, D. A. (2001). Activation, deactivation and adaptation in vertebrate photoreceptor cells. *Annual Review of Neuroscience*, *24*, 779–805. [[PubMed](#)]
- Chen, C. K., Burns, M. E., He, W., Wensel, T. G., Baylor, D. A., & Simon, M. I. (2000). Slowed recovery of rod photoresponse in mice lacking the GTPase accelerating protein RGS9-1. *Nature*, *403*, 557–560. [[PubMed](#)]
- Cowan, C. W., Fariss, R. N., Sokal, I., Palczewski, K., & Wensel, T. G. (1998). High expression levels in cones of RGS9, the predominant GTPase accelerating protein of rods. *Proceedings of the National Academy of Sciences of the United States of America*, *95*, 5351–5356. [[PubMed](#)] [[Article](#)]
- De Lange, H. (1958). Research into the dynamic nature of the human fovea-cortex systems with intermittent and modulated light: I. Attenuation characteristics with white and colored light. *Journal of the Optical Society of America*, *48*, 777–784.
- Fain, G. L., Matthews, H. R., Cornwall, M. C., & Koutalos, Y. (2001). Adaptation in vertebrate photoreceptors. *Physiological Reviews*, *80*, 117–151. [[PubMed](#)] [[Article](#)]
- Hamer, R. D., Nicholas, S. C., Tranchina, D., Lamb, T. D., & Jarvinen, J. L. (2005). Toward a unified model of vertebrate rod phototransduction. *Visual Neuroscience*, *22*, 417–436. [[PubMed](#)] [[Article](#)]
- He, W., Cowan, C. W., & Wensel, T. G. (1998). RGS9, a GTPase accelerator for phototransduction. *Neuron*, *20*, 95–102. [[PubMed](#)] [[Article](#)]
- Hecht, S., & Schlaer, S. (1936). Intermittent stimulation by light: V. The relation between intensity and critical frequency for different parts of the spectrum. *Journal of General Physiology*, *19*, 965–977.
- Hecht, S., & Verrijp, C. D. (1933). The influence of intensity, color and retinal location on the fusion frequency of intermittent illumination. *Proceedings of the National Academy of Sciences of the United States of America*, *19*, 522–535. [[PubMed](#)] [[Article](#)]
- Hodgkin, A. L., & Nunn, B. J. (1988). Control of light-sensitive current in salamander rods. *The Journal of Physiology*, *403*, 439–471. [[PubMed](#)] [[Article](#)]
- Hu, G., & Wensel, T. G. (2002). R9AP, a membrane anchor for the photoreceptor GTPase accelerating

- protein, RGS9-1. *Proceedings of the National Academy of Sciences of the United States of America*, 99, 9755–9760. [PubMed] [Article]
- Krispel, C. M., Chen, C. K., Simon, M. I., & Burns, M. E. (2003). Prolonged photoresponses and defective adaptation in rods of Gb5^{-/-} mice. *Journal of Neuroscience*, 23, 6965–6971. [PubMed] [Article]
- Lyubarsky, A. L., Naarendorp, F., Zhang, X., Wensel, T. G., Simon, M. I., & Pugh, E. N., Jr. (2001). RGS9-1 is required for normal inactivation of mouse cone phototransduction. *Molecular Vision*, 7, 71–78. [PubMed] [Article]
- Makino, E. R., Handy, J. W., Li, T., & Arshavsky, W. (1999). The GTPase activating factor for transducin in rod photoreceptors is the complex between RGS9 and type 5 G protein β subunit. *Proceedings of the National Academy of Sciences of the United States of America*, 96, 1947–1952. [PubMed] [Article]
- Marks, L. E., & Bornstein, M. H. (1973). Spectral sensitivity by constant CFF: Effect of chromatic adaptation. *Journal of the Optical Society of America*, 63, 220–226. [PubMed]
- Nikonov, S., Engheta, N., & Pugh, E. N., Jr. (1998). Kinetics of recovery of the dark-adapted salamander rod photoresponse. *Journal of General Physiology*, 111, 7–37. [PubMed] [Article]
- Nikonov, S., Lamb, T. D., & Pugh, E. N., Jr. (2000). The role of steady phosphodiesterase activity in the kinetics and sensitivity of the light-adapted Salamander rod photoresponse. *Journal of General Physiology*, 116, 795–824. [PubMed] [Article]
- Nishiguchi, K. M., Sandberg, M. A., Kooijman, A. C., Martemyanov, K. A., Pott, J. W. R., Hagstrom, S. A., et al. (2004). Defects in RGS9 or its anchor protein R9AP in patients with slow photoreceptor deactivation. *Nature*, 427, 75–78. [PubMed]
- Perlman, I., & Normann, R. A. (1998). Light adaptation and sensitivity controlling mechanisms in vertebrate photoreceptors. *Progress in Retinal and Eye Research*, 17, 523–563. [PubMed]
- Pokorny, J., Smith, V. C., & Lutze, M. (1988). Aging of the human lens. *Applied Optics*, 26, 1437–1440.
- Pugh, E. N., Jr. (1976a). Rhodopsin flash photolysis in man. *The Journal of Physiology*, 248, 393–412. [PubMed] [Article]
- Pugh, E. N., Jr. (1976b). Rushton's Paradox: Rod dark adaptation after flash photolysis. *The Journal of Physiology*, 248, 413–431. [PubMed] [Article]
- Pugh, E. N., Jr., & Lamb, T. D. (2000). Phototransduction in vertebrate rods and cones: Molecular mechanisms of amplification, recovery and light adaptation. In D. G. Stavenga, W. J. de Grip, & E. N. Pugh (Eds.), *Handbook of biological physics: Vol. 3. Molecular mechanisms of visual transduction* (pp. 183–255). Amsterdam: Elsevier.
- Pugh, E. N., Jr., Nikonov, S., & Lamb, T. D. (1999). Molecular mechanisms of vertebrate photoreceptor light adaptation. *Current Opinion in Neurobiology*, 9, 410–418. [PubMed]
- Rushton, W. A. H. (1972). Visual pigments in man. In H. J. A. Dartnall (Ed.), *Handbook of sensory physiology* (Vol. VII/1). New York: Springer-Verlag.
- Stockman, A., Langendörfer, M., & Sharpe, L. T. (2007). Human S-cone light adaptation. *Journal of Vision*, 7(3):4, 4, 1–7, <http://journalofvision.org/7/3/4/>, doi:10.1167/7.3.4. [PubMed] [Article]
- Stockman, A., Langendörfer, M., Smithson, H. E., & Sharpe, L. T. (2006). Human cone light adaptation: From behavioral measurements to molecular mechanisms. *Journal of Vision*, 6(11):5, 1194–1213, <http://journalofvision.org/6/11/5/>, doi:10.1167/6.11.5. [PubMed] [Article]
- Stockman, A., MacLeod, D. I. A., & DePriest, D. D. (1991). The temporal properties of the human short-wave photoreceptors and their associated pathways. *Vision Research*, 31, 189–208. [PubMed]
- Stockman, A., MacLeod, D. I. A., & Lebrun, S. (1993). Faster than the eye can see: Blue cones respond to rapid flicker. *Journal of the Optical Society of America A: Optics and Image Science*, 10, 1396–1402. [PubMed]
- Stockman, A., & Plummer, D. J. (1998). Color from invisible flicker: A failure of the Talbot-Plateau law caused by an early “hard” saturating nonlinearity used to partition the human short-wave cone pathway. *Vision Research*, 38, 3703–3728. [PubMed]
- Stockman, A., Plummer, D. J., & Montag, E. D. (2005). Spectrally-opponent inputs to the human luminance pathway: Slow +M and -L cone inputs revealed by intense long-wavelength adaptation. *The Journal of Physiology*, 566, 61–76. [PubMed] [Article]
- Watson, A. B. (1986). Temporal sensitivity. In K. Boff, L. Kaufman, & J. Thomas (Eds.), *Handbook of perception and human performance* (vol. 1, pp. 6-1–6-43). New York: Wiley.
- West, S. K., Duncan, D. D., Muñoz, B., Rubin, G. S., Fried, L. P., Bandeen-Roche, K., et al. (1998). Sunlight exposure and risk of lens opacities in a population-based study. *Journal of the American Medical Association*, 280, 714–718. [PubMed] [Article]